New Maleic Anhydride Modified PP Copolymers with Block Structure: Synthesis and Application in PP/Polyamide Reactive Blends

Bing Lu and T. C. Chung*

Department of Materials Science and Engineering, The Pennsylvania State University, University Park, Pennsylvania 16802

Received January 4, 1999; Revised Manuscript Received February 25, 1999

ABSTRACT: This paper discusses a new class of maleic anhydride modified PP polymers (PP-MA), having a relatively well-defined molecular structure. The chemistry involves the borane-terminated PP intermediate that is prepared by hydroboration of the chain-end unsaturated PP. The borane group at the chain end was selectively oxidized by oxygen to form a "stable" polymeric radical which then in situ reacts with maleic anhydride to produce maleic anhydride terminated PP (PP-t-MA) with a single MA unit. In the presence of styrene, the polymeric radical initiated an alternative copolymerization of styrene and maleic anhydride to produce PP-*b*-SMA diblock copolymers, and the incorporated MA units are proportional to the concentration of styrene and the reaction time. No detectable side reaction was observed in the PP polymer chain. The resulting relatively well-defined PP-MA copolymers, with controllable PP molecular weight and MA concentration, were evaluated systematically in the reactive PP/PP-MA/polyamide blends. The compatibility is dependent on not only the microstructure of the compatibilizer, formed in situ by reacting PP-MA with polyamide chains, but also the composition of the PP/polyamide blend. In polyamide-rich blends, all PP-MA copolymers show limited compatibility. Higher MA concentrations result in poor blend morphologies. Most of the compatibilizers formed fail to position themselves at the interfaces between the PP and polyamide domains. On the other hand, in PP-rich blends the in situ formed compatibilizers are generally very effective, especially those involving the PP-*b*-SMA with high PP molecular weight and multiple MA units.

Introduction

Functionalization of polyolefins (i.e., PE, PP, etc.) has long been a scientific challenge and an industrial important research area,[1−4] which represents a route to expand polyolefin applications and to produce higher value products. By far, maleic anhydride (MA) modified polyolefins are the most important class of functionalized polyolefins in commercial applications due to their unique combination of low cost, high activity, and good processiblity. They are the general choice of material in improving compatibility, adhesion, and paintability of polyolefins. Among them, MA modified PP (PP-MA)[5] is the most investigated polymer and is used in applications, such as glass fiber reinforced PP,[6] anticorrosive coatings for metal pipes and containers,[7] metal−plastic laminates for structural use,[8] multilayer sheets of paper for chemical and food packaging,[9] and polymer blends.[10−12]

PP-MA was usually prepared by chemical modification of preformed PP under free radical conditions.[13,14] Due to the inert nature of the PP structure and poor control of the free radical reaction, this MA grafting reaction includes many undesirable side reactions,[15] such as β-scission, chain transfer, and coupling. The MA incorporation is usually inversely proportional to the resulting polymer molecular weight. In addition to the MA units incorporated along the polymer side chain, it has been generally suggested that a significant portion of PP-MA polymers have a succinic anhydride group located at the polymer chain end,[16,17] resulting from β-scission. In general, the inherent complexity of PP-MA molecular structure has significantly limited the understanding of its structure−property relationship, especially the ability of PP-MA as an interfacial agent in PP blends and composites.

In our previous communication,[18] we discussed a new synthetic route for preparing PP-MA copolymers, which involves the borane group terminated PP and a free radical graft-from reaction with maleic anhydride. The resulting PP-MA polymer containing a chain end terminated MA group was an effective compatibilizer in a PP/polyamide blend.

Results and Discussion

In this paper we will summarize the detailed experimental conditions and results in the synthesis of both PP-MA copolymers and the reactive PP/polyamide blends. The goal is to investigate the best reaction conditions to prepare the well-defined block copolymers, with controllable PP molecular weight and MA concentration and minimun byproducts. The other goal is to study the correlation of PP-MA molecular structures to the compatibility in the reactive PP/Polyamide blends. The availability of well-defined PP-MA copolymers offers an excellent opportunity to systematically compare the effects of PP-MA molecular structure on the reactive polymer blends.

Scheme 1 illustrates the steps involved in the preparation of PP-MA copolymers. The chain-end unsaturated PP (**I**) can be prepared by metallocene polymerization or thermal degradation of high molecular weight PP. Following the hydroboration reaction with 9-BBN (9-borabicycoborane) to obtain the borane terminated PP (**II**), the borane group at the chain end was selectively oxidized[19,20] by oxygen to form a polymeric radical (**III**) which is associated with a "stable" borinate radical.[21] The polymeric radical in situ reacts with maleic anhydride to produce maleic anhydride terminated PP (PP-

* To whom all correspondence should be addressed.

10.1021/ma990019q CCC: $18.00
Published on Web 03/26/1999

Scheme 1

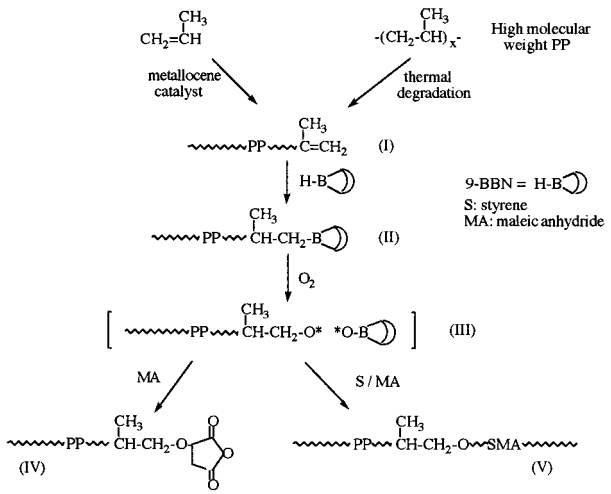

t-MA) (**IV**) with a single MA unit. In the presence of styrene, the polymeric radical initiates a "stable" copolymerization[22,23] of styrene and maleic anhydride with an alternative manner.[24] The resulting PP-*b*-SMA diblock copolymer (**V**) contains both PP and alternating styrene−maleic anhydride (SMA) segments.

Chain-End Unsaturated PP. The first step in the preparation of chain end unsaturated PP (u-PP) polymers involves the metallocene polymerization of propylene with the predominated termination reaction by β-hydrogen elimination.[25] Two of the most common isospecific metallocene catalysts, i.e., {$SiMe_2$[2-Me-5-Ph-(Ind)]$_2$}$ZrCl_2$ (A) and Et(Ind)$_2$$ZrCl_2$ (B), were studied under various reaction conditions. In general, the catalyst A, with highly isospecific coordination and suppressed β-hydrogen elimination, produces high molecular weight PP with concentrations of olefinic units below the detectable level in all reaction conditions. On the other hand, catalyst B clearly shows the termination proceeding with β-hydrogen elimination. The higher the polymerization temperature, the lower the molecular weight of the polymer and the higher the chain-end unsaturation concentration. As summarized in Table 1, the resulting u-PP-1 and u-PP-2 polymers have narrow molecular distributions and relatively low melting temperatures (T_m < 140 °C).

The other method of producing u-PP is a thermal degradation process[26] which was carried out by mixing a molten Ziegler−Natta PP polymer (with high molecular weight and $T_m \sim 164$ °C) with a high-temperature decomposed peroxide reagent (proton-extraction agent) in a Brabender mixer. The thermal degradation reaction is believed to follow the removal of a tertiary proton in the PP backbone by a peroxyl radical. As shown in Table 1, the degradation reaction is very effective, even with relatively low concentrations of peroxide and a low reaction temperature. The polymer chain was degraded 10 times on average in 8 min.

The molecular weight of the resulting polymer is inversely proportional to the peroxide concentration and reaction time. Figure 1 compares GPC curves of the initial PP and the resulting u-PP polymers.

With increasing chain degradation, the molecular weight distribution of the u-PP is gradually reduced—an indication of the statistic degradation process.

The chain-end vinylidene group can be detected by an IR spectrum with a weak absorption peak at 888 cm^{-1} as shown in Figure 2.

It is very difficult to quantify this olefin concentration based on the peak intensity alone, especially for high molecular weight polymers. However, it was reported that each thermal degradation generates a vinylidene unit[27] at one broken chain end. Statistically, the product is a mixture, containing predominately PP chains with one vinylidene chain-end unit, some PP chains having both vinylidene chain-end units, and only a few PP chains without a vinylidene group, especially after an extended degradation reaction. The percentage of PP chains without vinylidene group will be discussed in the chain extension reaction.

PP-t-MA and PP-b-SMA. The vinylidene group at the u-PP chain end can be effectively hydroborated by a 9-borabicyclononane (9-BBN) reagent in suspension, by stirring the u-PP powder with a slight excess of 9-BBN in THF at 55 °C for 5 h. On the basis of our previous experimental results,[28] the reaction is almost quantitative, due to very high hydroboration reactivity and the high surface area of reaction sites. The borane terminal group was then selectively oxidized by oxygen to form a "stable" polymeric alkoxyl radical (associated with the boroxyl radical), which then initiates a free radical reaction of maleic anhydride both with and without the presence of styrene. Due to MA's low tendency for homopolymerization,[29] a very low concentration of MA (possibly only a single MA unit) was incorporated in the PP structure to form MA terminated PP (PP-t-MA). On the other hand, with the presence of styrene in the PP-B/MA mixture, the free radical graft-from polymerization takes place to extend the PP chain end with an alternating styrene and MA (SMA) copolymer.[20] In other words, a diblock copolymer PP-*b*-SMA is obtained, containing both PP and SMA segments. The MA concentration in the copolymer is governed by the molecular weight of the SMA segment.

Figure 3 compares the ^{1}H NMR spectra of the initial u-PP-2, the corresponding PP-2-t-MA, and the reaction product of PP-2-t-MA and 3-aminopropyltrimethoxysilane.

In Figure 3a, the u-PP sample shows three multiple peaks around 0.95, 1.35, and 1.65 ppm, corresponding to C**H**$_3$, C**H**$_2$, and C**H** protons, which are accompanied by two singlets at 4.7 and 4.8 ppm, corresponding to two vinylidene protons at the chain end. As shown in Figure 3b, both olefinic proton peaks are completely beyond the limits of NMR sensitivity after hydroboration and MA graft-from reactions. However, there is no chemical shift corresponding to the methylene and methine protons of the terminal MA units, which may be due to the long relaxation time of the MA group in the hydrocarbon polymer. It is interesting to note that the MA end group in PP-t-MA can be revealed by further imidization reactions of succinic anhydride groups with a 3-aminopropyltrimethoxysilane reagent. As shown in Figure 3c, two new peaks appear at 3.48 and 3.72 ppm, corresponding to Si(OCH_3)$_3$ and N−CH_2. The integrated intensity ratio of the chemical shifts at 3.48 ppm and the chemical shift between 0.9 and 1.9 ppm, and the number of protons both chemical shifts represent, indicates more than 80% of PP chains containing a terminal MA group. Apparently, both hydroboration and oxidation reactions were not inhibited by the insolubility of polypropylene, and the MA end group in PP-t-MA is very reactive to the primary amino group. It is interesting to note that the same chemical reaction also involves the PP/polyamide reac-

Table 1. A Summary of Chain-End Unsaturated PP Polymers

	preparation condition				product properties			
sample no.	method	catalyst	temp (°C)	time (min)	$M_v \times 10^4$	$M_w \times 10^4$	M_w/M_n	T_m (°C)
uPP-1	polymerization[a]	5×10^{-6} mol [Zr]	50	60	1.2	1.6	1.4	121.1
uPP-2	polymerization[a]	5×10^{-6} mol [Zr]	30	60	3.8	4.2	1.6	138.7
uPP-3[b]					1.4	1.5	2.5	155.2
uPP-4	degradation[c]	peroxide,[d] 1.6 g	180	8	5.3	6.2	2.7	145.4
uPP-5	degradation[c]	peroxide,[d] 0.8 g	180	8	5.9	7.8	3.0	153.7
uPP-6	degradation[c]	peroxide,[d] 0.8 g	180	6	6.7	10	3.2	160.1
uPP-7	degradation[c]	peroxide,[d] 0.8 g	180	4	11	16	4.3	161.9
uPP-8	degradation[c]	peroxide,[d] 0.4 g	180	4	14	20	4.8	162.6
uPP-9	degradation[c]	peroxide,[d] 0.2 g	180	4	16	26	5.4	162.3

[a] Polymerization: 100 mL of toluene, 5 μmol of $EtInd_2ZrCl_2$, Al/Zr = 500, propylene pressure 10 psi. [b] Obtained from Aldrich Chemical Co. [c] Degradation: in a Brabender Plasticorder mixer, the starting PP polymer ($M_v = 4.8 \times 10^5$, $M_w = 5.9 \times 10^5$, $M_w/M_n = 6.6$, $T_m = 163.7$ °C). [d] Peroxide: 2,5-bis(*tert*-butylperoxy)-2,5-dimethyl-3-hexyne.

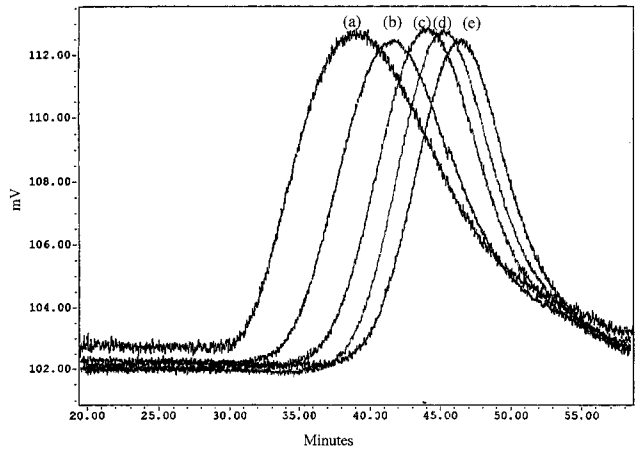

Figure 1. GPC curves of (a) starting PP and the thermally degraded PP (b) u-PP-9, (c) u-PP-7, (d) u-PP-6, and (e) u-PP-4 polymers.

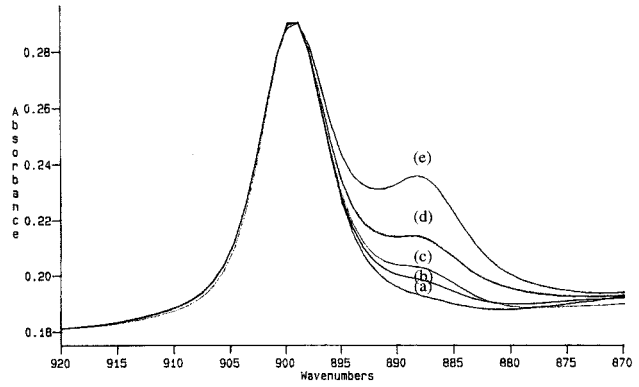

Figure 2. IR spectrum of (a) starting PP and the thermally degraded PP (b) u-PP-9, (c) u-PP-7, (d) u-PP-6, and (e) u-PP-4 polymers.

tive blends which will be discussed later. The efficiency of the reaction must be due to the high surface area of the reactive sites. While some of the polypropylene segments are crystallized, the polymer chain ends are expelled into the amorphous phase which can be swelled by using an appropriate solvent during the reaction. In addition, the high reactivities in hydroboration, oxidation, and imidization reactions certainly enhance the efficiency of functionalization.

Figure 4 compares IR spectra of the initial u-PP-2 and three corresponding PP-2-*b*-SMA copolymers that were prepared with the same reagents and different reaction times.

After the SMA graft-from reaction, several new absorption peaks were observed at 1860 and 1780 cm^{-1}, corresponding to two $\upsilon_{C=O}$ vibrational stretching modes in succinic anhydride, at 900−950 cm^{-1}, corresponding to the υ_{C-H} deformation in succinic anhydride, and at 700, 750, and 580 cm^{-1}, corresponding to styrene υ_{C-H} deformation. It is clear that a very high concentration of MA groups have been incorporated with styrene units in the PP-*b*-SMA block copolymer and that the molecular weight of the SMA segment is basically proportional to the reaction time. The concentration of incorporated MA units was calculated by a standard industrial method[30] (discussed in the Experimental Section) that is based on the IR carbonyl group absorption intensity and sample thickness.

Table 2 summarizes the experimental results of four comparative reaction sets which includes four different initial u-PP polymers with various molecular weights and melting points. In each set, the experimental results are compared under various reaction conditions. In most cases, the reaction mixture isolated by filtration was subjected to Soxhlet extraction with refluxing xylene and acetone for 24 h to remove unreacted PP and ungrafted SMA, respectively. In some cases, such as PP-2-*b*-SMA-1 containing less than 3 wt % MA, the reaction mixtures were only subjected to acetone to remove the ungrafted SMA polymer, due to the similar solubility of unreacted PP and PP-MA. In general, the graft efficiency was very high, and the major portion (>80%) of u-PP was converted to PP-*b*-SMA diblock copolymer. Some unreacted PP polymers (<20%) may due to their completely saturated molecular structure, obtained during metallocene polymerization and thermal degradation reactions. This observation is quite consistent with the previous ^1H NMR results of the imidized PP-t-MA, which also indicated about 80% of the initial u-PP chains containing a vinylidene group. Some ungrafted SMA polymers were also isolated. It is very interesting to note that this undesirable side reaction can be minimized by lowering the reaction temperature (in the PP-2-*b*-SMA-5 and PP-4-*b*-SMA-5 cases) or adding some free-radical inhibitors (in the PP-2-*b*-SMA-6 and PP-4-*b*-SMA-6 cases). Apparentally, the active site responsible for the ungrafted SMA polymers is basically a traditional free radical initiation site, sensitive to temperature and inhibitors, and the one responsible for the graft-from reaction is a "stable" initiation site (**III**) shown in Scheme 1, which is insensitive to the reaction temperature and inhibitor.

In detail, all four PP-t-MA copolymers shall have above 80% of polymer chains containing a terminal MA unit, about 0.3, 0.8, 0.2, and 0.06 wt % of MA in PP-2-t-MA, PP-3-t-MA, PP-4-t-MA, and PP-9-t-MA samples, respectively. With the addition of styrene, the incorpo-

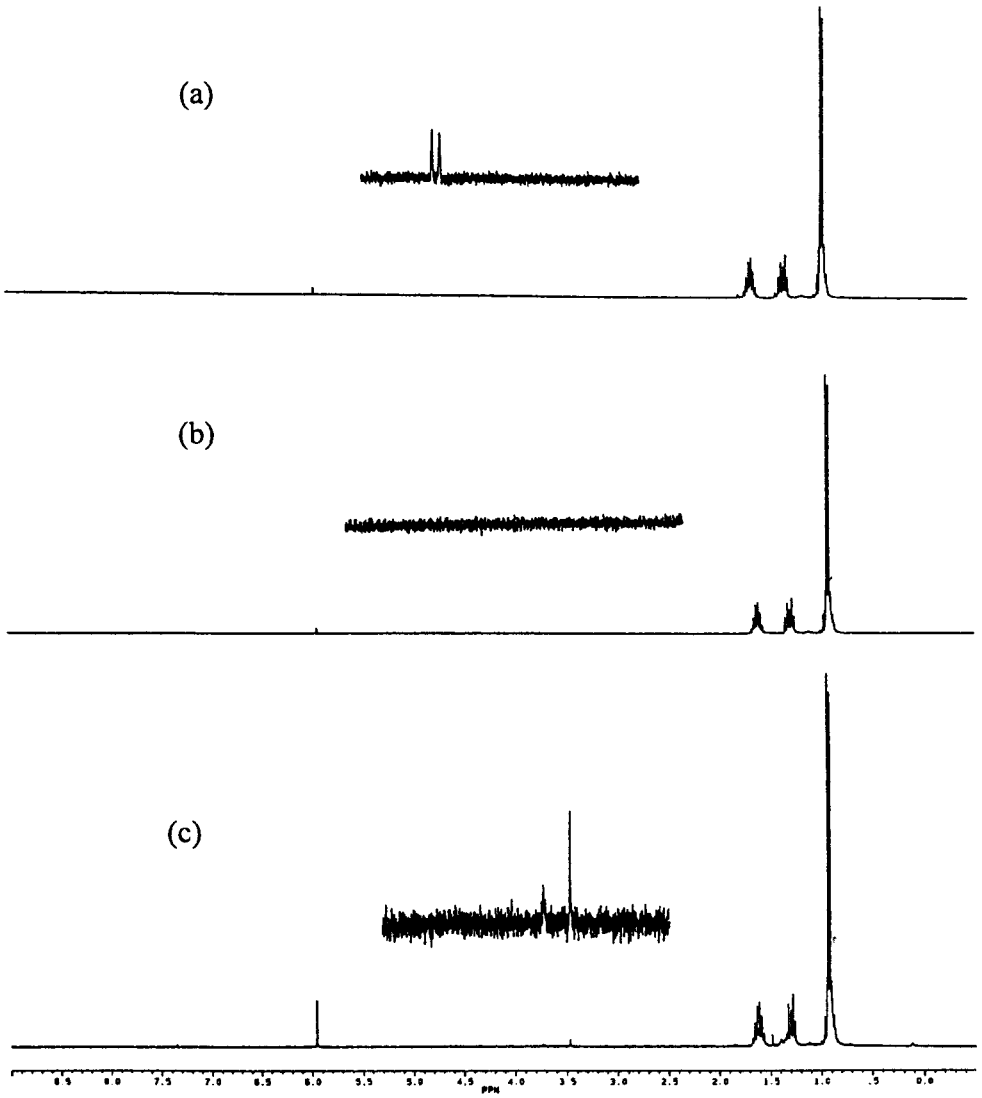

Figure 3. ^{1}H NMR spectra of (a) starting u-PP-2, (b) the corresponding PP-2-t-MA, and (c) the reaction product of PP-2-t-MA and 3-aminopropyltrimethoxysilane.

ration of MA units dramatically increases, and the concentration is dependent on the styrene concentration (comparing samples PP-4-*b*-SMA-1 and PP-4-*b*-SMA-2) and reaction time (comparing samples PP-4-*b*-SMA-2 and PP-4-*b*-SMA-3). In the PP-4-*b*-SMA-3 sample, 25 wt % MA incorporation indicates about 50 wt % of SMA, assuming that an alternating copolymer segment existed in this diblock copolymer. In other words, the molecular weight of the SMA segment is about 5.3×10^4 g/mol, similar to that of PP segment. Similar results were observed in other reaction sets. Despite the initial very high molecular weight (1.63×10^5 g/mol) of the u-PP-9 polymer and thus the extremely low concentration of reactive sites, the chain extension took place and the amount of incorporated MA units dramatically increased. IR spectra also show that the concentration of MA also increases with higher styrene concentration and reaction times (comparing samples PP-9-*b*-SMA-1 and PP-9-*b*-SMA-2). Sample PP-9-*b*-SMA-2 contains a high concentration (20 wt %) of MA units with the estimated molecular weight $>2.6 \times 10^5$ g/mol, assuming alternating SMA segment in the diblock copolymer.

With the increase of SMA concentration in the PP structure, the solubility of the polymer is gradually reduced. Only the samples containing MA units <1.5 wt % are soluble in decalin for molecular weight determination. However, all the samples are melt processible at 260 °C. It is very interesting to note that all measured PP-t-MA and PP-*b*-SMA samples (soluble in decalin) show molecular weights similar to the initial u-PP, indicating that no detectable degradation or cross-linking reactions happened during MA grafting reactions. This is a great departure from the current maleic anhydride modified PP technology.

Figure 5 compares three DSC curves of uPP-2, PP-2-*b*-SMA-1, PP-2-*b*-SMA-2, and PP-2-*b*-SMA-3 in the first reaction set discussed in Table 2. An almost identical melting peak near 140 °C, corresponding to T_m of the PP polymer, was observed in all samples. A clear new T_g at about 216 °C (corresponding to the alternating SMA copolymer[5]) was shown in the PP-2-*b*-SMA-3 sample. Two thermal transitions almost identical to those of the two corresponding PP and SMA polymers indicate phase separation between the PP and SMA domains. Both polymer segments in the diblock copolymer must have long consecutive (undisturbed) sequences to form separate domains.

PP/Nylon Blends. These PP-t-MA and PP-*b*-SMA copolymers with relatively well-defined structures were used as the compatibilizers in the reactive PP/polyamide

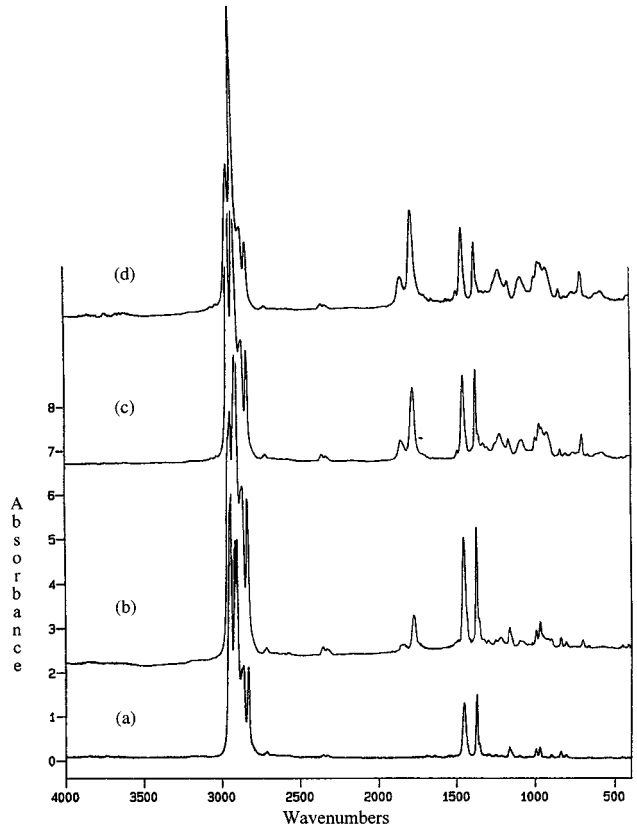

Figure 4. Comparison of IR spectra, (a) the starting u-PP-2, (b) PP-2-*b*-SMA-1, (c) PP-2-*b*-SMA-2, and (d) PP-2-*b*-SMA-3.

blends, containing PP (M_w = 288 000 and M_n = 43 300 g/mol) and Nylon 11 (M_n = 24 800 g/mol). The reactive mixing was carried out in a Brabender mixer at 220 °C for 20 min. Ideally, the PP-t-MA and PP-*b*-SMA copolymers would react with Nylon 11 in situ right at the interfaces between the PP and Nylon 11 domains and produce a PP-*b*-Nylon 11 block copolymer and a PP-*g*-Nylon 11 graft copolymer with "brushlike" microstructure, respectively, as illustrated in Scheme 2. The polymer blend's morphology was examined by observing the surface topography of cold fractured film edges using scanning electron microscopy. Figure 6 shows SEM photographs of two homopolymer blends, including a PP-rich blend (PP/Nylon 11 = 75/25 wt %) and a Nylon 11-rich blend (PP/Nylon 11 = 25/75 wt %).

In both homopolymer blends, the polymers are grossly phase separated as can be seen by the minor component Nylon 11 and PP in Figure 6, a and b, respectively, which show nonuniform, poorly dispersed domains and voids at the fracture surface. This "ball-and-socket" topography is indicative of poor interfacial adhesion between the PP and Nylon domains and represents minor component domains that are pulled out of the major component matrix. Such pull out indicates that no stress transfer takes place between phases during fracture.

The introduction of the PP-t-MA compatibilizer, containing only one reactive MA unit at the chain end, into the PP/Nylon11 blend is expected to in situ form PP-*b*-Nylon 11 diblock copolymer (as discussed in Scheme 2) which serves as a compatibilizer at the PP/Nylon interfaces. Figures 7 and 8 compare two sets of ternary PP/PP-t-MA/Nylon 11 blendings, including a PP-rich system (PP/PP-t-MA/Nylon 11 = 70/5/25 wt %) and a Nylon-rich system (PP/PP-t-MA/Nylon 11 = 20/5/75 wt %). The magnification is 1500×.

With 5 wt % of PP-t-MA copolymer, the compatibility of the PP/Nylon 11 blends is generally improved. Unexpectedly, both systems show that the compatibility is inversely proportional to the PP molecular weight of the PP-t-MA copolymer. The higher the PP molecular weight, the lower the compatibility. In Figures 7a and 8a, the PP-3-t-MA copolymer having a low molecular weight (M_w = 15 000 and M_n = 6000 g/mol) and T_m (~155 °C) shows a quite effective compatibility in both PP-rich and Nylon 11-rich blends. No distinct phases are observable, indicating that fracture occurred through both phases or that the minor phase is too small to be observed. The results imply effective cocrystallization between the high molecular weight PP (M_w = 288 000 and M_n = 43 300) and the low molecular weight PP segment (M_w = 15 000 and M_n = 6000) of PP-t-MA. A small difference in the melting points of the two PP segments seems to have a minimum effect on the cocrystallization process. On the other hand, the concentration of the reactive MA unit in the PP-t-MA is important. A certain MA concentration is necessary to secure the PP-t-MA and Nylon 11 in situ reaction. Figure 7c only shows very limited compatibility in the PP/Nylon blend by using a PP-9-t-MA compatibilizer having a high PP molecular weight (M_w = 260 000 and M_n = 48 000) and a very low MA concentration.

The side-by-side comparisons between Figure 7b and Figure 8b and between Figure 7c and Figure 8c show significantly better compatibility of PP-t-MA in the PP-rich blends than in the corresponding Nylon 11-rich blends. The clear pulled out "ball-and-socket" topography in Figure 8b,c is indicative of poor interfacial adhesion between the PP discrete phases and the Nylon 11 matrix. Some of PP-*b*-Nylon 11 diblock copolymer formed in situ in the Nylon-rich system may have a tendency to form separate domains within the Nylon matrix, which may significantly reduce the effectiveness of the PP-t-MA copolymer. The same tendency was very clearly observed in some PP-*b*-SMA cases, containing multiple MA units, which will be discussed below.

It is very interesting to study the PP-*b*-SMA copolymer in the PP/Nylon blend. The copolymer contains multiple reactive MA units at the PP chain end and will form the compatibilizer of the PP-*g*-Nylon graft copolymer with "brushlike" structure (as shown inScheme 2). Figures 9 and 10 compare SEM micrographs of both the PP-rich system (with PP/PP-*b*-SMA/Nylon 11 = 70/5/25 wt %) and the Nylon 11-rich system (with PP/PP-*b*-SMA/Nylon 11= 20/5/75 wt %), respectively. It is very unexpected to observe the completely opposite results in these two systems. The PP-*b*-SMA copolymer shows almost no appreciable benefit to the Nylon 11-rich blends. On the other hand, PP-*b*-SMA shows very good compatibility in the PP-rich blends, and the higher the molecular weight, the better the compatibility. It is logical to expect that the increase of MA units in the PP-*b*-SMA copolymer increases the graft density of the Nylon 11 side chains in the PP-*g*-Nylon 11 compatibilizer. The multiple Nylon 11 chains in the PP-*g*-Nylon 11 may increase its hydrogen-bonding interactions with the Nylon 11 homopolymers, particularly in the Nylon-rich blend environment. The surge of hydrogen-bonding energy may overwhelm the cocrystallization energy between the PP-*g*-Nylon 11 and the PP. Such a thermodynamic inbalance at two interfaces, i.e., Nylon/PP-*g*-Nylon and PP-*g*-Nylon/PP, may increase the tendency

Table 2. A Summary of Maleic Anhydride Modified PP Copolymers

	preparation conditions[a]			fractionation results			product properties			
sample no.	styrene (mL)	temp (°C)	time (h)	W_{SMA} (g)	W_{PP} (g)	$W_{diblock}$ (g)	$M_v \times 10^4$	MA (wt %)	T_m (°C)	T_g (°C)
uPP-2							3.8	0	138.7	
PP-2-t-MA	0	45	4				3.8	0.3	138.2	
PP-2-*b*-SMA-1	2	45	1	0.124		1.053	3.9	5.1	138.0	
PP-2-*b*-SMA-2	2	45	4	0.350	0.113	1.426		16	138.9	216
PP-2-*b*-SMA-3	2	45	16	0.548	0.106	2.083		26	140.3	213
PP-2-*b*-SMA-4	2	20	16	0.137	0.109	1.622		20	139.1	214
PP-2-*b*-SMA-5	2	0	16	0.076	0.108	1.485		19	138.6	213
PP-2-*b*-SMA-6[b]	3	20	16	0.070	0.112	1.432		18	138.2	213
uPP-3							1.4	0	155.2	
PP-3-t-MA	0	45	4				1.4	0.8	155.6	
PP-3-*b*-SMA-1	0.1	45	4				1.6	1.5	155.4	
uPP-4							5.3	0	145.4	
PP-4-t-MA	0	45	4				5.4	0.2	146.8	
PP-4-*b*-SMA-1	0.1	45	4				5.4	1.1	147.2	
PP-4-*b*-SMA-2	2	45	4	0.302	0.134	1.274		9.6	146.5	213
PP-4-*b*-SMA-3	2	45	10	0.510	0.130	2.014		25	146.1	212
PP-4-*b*-SMA-4	2	20	10	0.146	0.124	1.443		16	146.3	213
PP-4-*b*-SMA-5	2	0	10	0.035	0.131	1.407		14	146.5	213
PP-4-*b*-SMA-6[b]	2	20	10	0.045	0.128	1.411		14	146.7	213
uPP-9							16	0	162.3	
PP-9-t-MA	0	45	4				16	0.06	162.6	
PP-9-*b*-SMA-1	0.1	45	4				16	1.0	163.4	
PP-9-*b*-SMA-2	2	45	10	0.506	0.193	1.658		20	162.6	216

[a] 1 g of borane-terminated PP, 2 g of maleic anhydride, 20 mL of benzene. [b] Adding 0.01 g of pentaerythritol tetrakis(3,5-di-*tert*-butyl-4-hydroxyhydrocinnamate) inhibitor in the reaction solution.

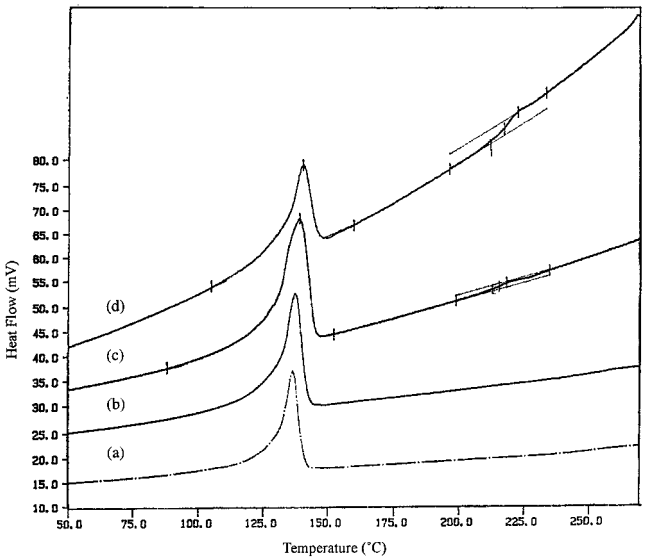

Figure 5. Comparison of three DSC curves of (a) u-PP-2, (b) PP-2-*b*-SMA-1, (c) PP-2-*b*-SMA-2, and (d) PP-2-*b*-SMA-3.

Scheme 2

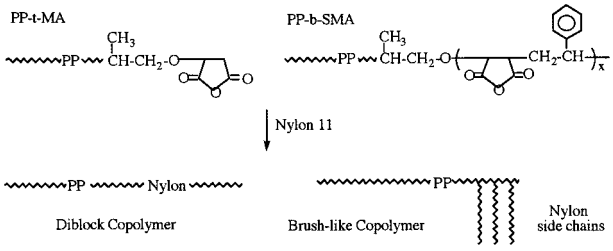

of PP-*g*-Nylon to form discrete domains by itself in the continuous Nylon 11 matrix. Therefore, the compatibility is largely lost (as shown in Figure 10). On the other hand, in the PP-rich system (in Figure 9) the formed "brushlike" PP-*g*-Nylon 11 compatibilizer may mostly stay at the interfaces, due to the balanced energy between the effective cocrystallization of the PP (continuous major phases) and the PP segment of PP-*g*-

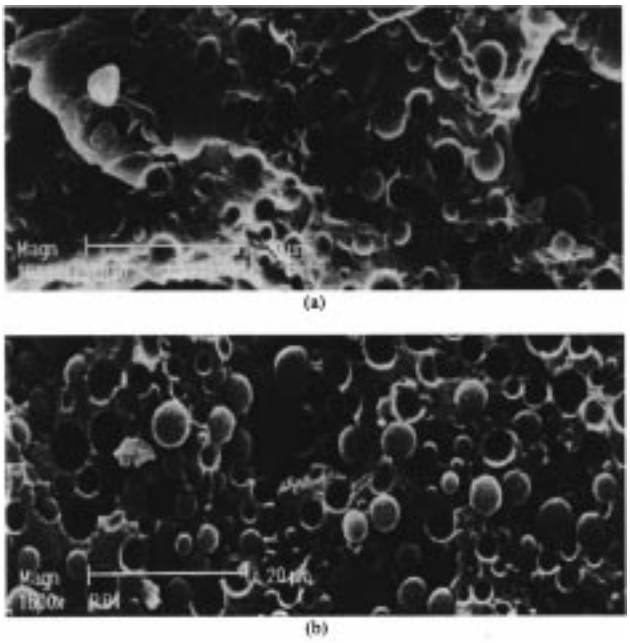

Figure 6. SEM photographs of two homopolymer blends, including (a) a PP-rich blend (PP/Nylon 11 = 75/25 wt %) and (b) a Nylon-rich blend (PP/Nylon 11 = 25/75 wt %).

Nylon 11 and the interactions of Nylon 11 (discrete minor phases) and the multiple Nylon 11 side chains of the PP-*g*-Nylon 11. This phenomenon is particularly clear in the ternary blends involving PP-9-*b*-SMA with high PP molecular weight. Figure 10c shows the "ball-and-socket" topography in the Nylon 11-rich blend. On the other hand, Figure 9c displays no distinct globules in the corresponding PP-rich blend. Rather, a flat mesalike fracture surface is observed similar to that seen on a fractured PP homopolymer. Both the PP and Nylon phases must be mechanically tied.

It is very interesting to compare Figure 9c and Figure 7c. Both have similar ternary PP-rich blends and the same high molecular weight of PP segment in PP-9-t-

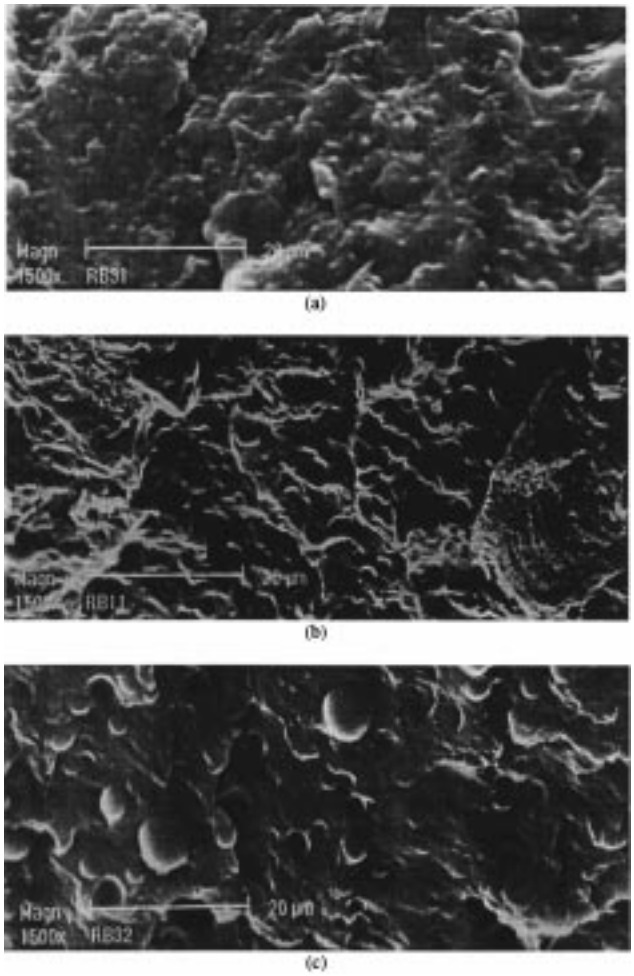

Figure 7. Comparison of three ternary PP/PP-t-MA/Nylon 11 = 70/5/25 wt % blends, including (a) PP/PP-3-t-MA/Nylon 11, (b) PP/PP-t-MA/Nylon 11, and (c) PP/PP-9-t-MA/Nylon 11. The magnification is 1500×.

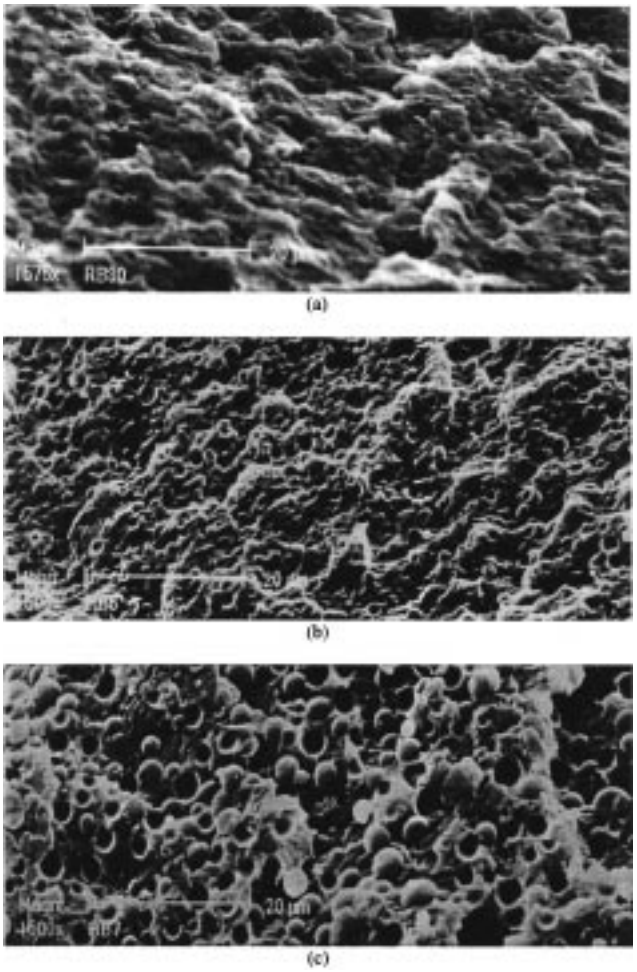

Figure 8. Comparison of three ternary PP/PP-t-MA/Nylon 11 = 20/5/75 wt % blends, including (a) PP/PP-3-t-MA/Nylon 11, (b) PP/PP-4-t-MA/Nylon 11, and (c) PP/PP-9-t-MA/Nylon 11. The magnification is 1500×.

MA and PP-9-*b*-SMA-1 compatibilizer structures. The only difference is the number of MA units (1 vs ∼10 MA units) located at the PP chain end. Comparison of the two micrographs clearly shows the advantage of high MA content in the high molecular weight PP-9-*b*-SMA-1 compatibilizer which can form strong interactions with both PP continuous and Nylon 11 discrete phases. The high overall cocrystallization energy (due to the high PP molecular weight) may balance it out with the mutiple interactions with the Nylon 11. Therefore, two strong and balanced PP/PP-9-*b*-SMA-1 and PP-9-*b*-SMA-1/Nylon 11 interactions secure the PP and Nylon 11 interfaces.

Experimental Section

Instrumentation and Materials. All high-temperature ^{1}H NMR spectra were recorded on a Bruker AM-300 spectrometer. Fourier transform infrared spectroscopy was performed on a Bio-Rad instrument using a polymer thin film. The MA concentration in the polymer was estimated with the following equation: MA wt % = $(k_1A_{1780cm^{-1}} + k_2A_{1710cm^{-1}})/d$, where d is the film thickness, $A_{1780cm^{-1}}$ and $A_{1710cm^{-1}}$ are the peak absorbencies and k_1 and k_2 are the absorption constants for anhydride and acid, respectively. Both k_1 and k_2 were determined by calibration of the known commercial compounds (Uniroyal), assuming the absorption constants are independent of the incorporated MA structures. Differential scanning calorimetry was measured on a Perkin-Elmer DSC-7 instrument controller, from 0 to 300 °C with a heating rate of 20 °C/min. The molecular weight and molecular weight distribution of the u-PP polymers were determined by gel permeation chromatography (GPC) using a Waters 150 C with a refractive index (RI) detector and a set of u-Styragel HT columns of 10^6, 10^5, 10^4, and 10^3 pore size in series. The measurements were taken at 140 °C using 1,2,4-trichlorobenzene (TCB) as solvent and a mobile phase of 0.7 mL/min flow rate. Broad molecular weight PE samples were used as standards for calibration. The viscosities of polymer solutions in decahydronaphthalene (decalin) inhibited with BHT were determined at 135 °C with a Cannon-Ubbelohde viscometer. The viscosity molecular weight was calculated by the Mark−Houwink equation: $[\eta] = KM_v^a$ where $K = 1.05 \times 10^{-5}$ and $a = 0.80$.[31]

9-BBN, maleic anhydride, styrene, THF, and *rac*-$Et_2Ind_2ZrCl_2$ were purchased from Aldrich Chemical Co. Me_2Si(2-methyl-4-phenylindine)$_2ZrCl_2$ and methylaluminoxane (MAO) 30 wt % toluene solution were purchased from Boulder Scientific and Ethyl Chemical Corp., respectively. Maleic anhydride was purified by sublimation before use. Styrene was vacuum distilled after drying with CaH_2. THF was distilled after drying with CaH_2 and sodium. Propylene gas (MG Industries) was used as received. HPLC grade THF and toluene were deoxygenated by argon spurge before refluxing for 48 h and then distilling from their respective green or purple sodium anthracide solution under argon. 2-Propanol was refluxed in CaH_2 before distilling under argon. All three solvents were stored in the drybox.

Preparation of u-PP by Metallocene Polymerization. In a typical reaction, the polymerization of propylene was carried out in a 450 mL Parr stainless autoclave equipped with a mechanical stirrer. A 100 mL aliquot of anhydrous toluene

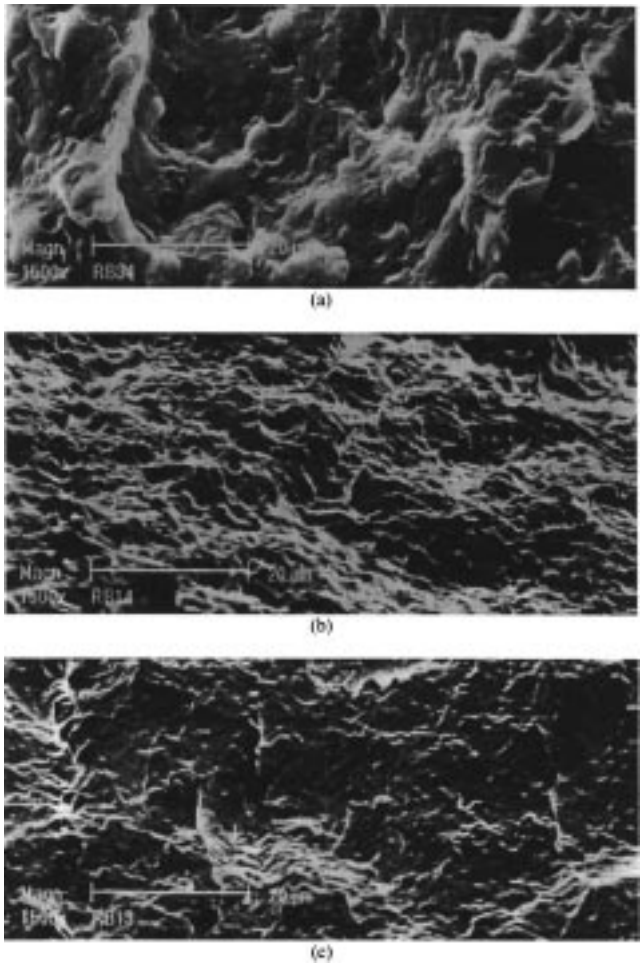

Figure 9. Comparison of three ternary PP/PP-*b*-SMA/Nylon 11 = 70/5/25 wt % blends, including (a) PP/PP-3-*b*-SMA-1/Nylon 11, (b) PP/PP-4-*b*-SMA-1/Nylon 11, and (c) PP/PP-9-*b*-SMA-1/Nylon 11. The magnification is 1500×.

and 2.5 mmol of MAO solution in toluene were injected into the reactor under argon atmosphere. The reactor was then connected to a propylene gas source and purged with 10 psi of propylene gas for a few minutes while the temperature was set to a preset value. When the temperature reached the preset temperature (30, 50, or 80 °C), 5.0 μmol of $Et(Ind)_2ZrCl_2$ solution in toluene was injected into the reactor under a propylene gas atmosphere to initiate the polymerization. The propylene gas pressure was maintained constantly at 10 psi throughout the reaction. After 1 h, the polymerization was terminated by releasing the propylene gas and adding 100 mL of dilute HCl solution in methanol. The polymer was then isolated by further washing with methanol, filtration, and drying at 50 °C in a vacuum oven.

Preparation of u-PP by Thermal Degradation. The thermal degradation of PP was carried out in a Brabender PL2000 mixer. About 40 g of PP powder (M_w = 580 000, M_n = 166 000, $T_m \sim$ 164 °C) was mixed with various quantities (shown in Table 1) of 2,5-bis(*tert*-butylperoxy)-2,5-dimethyl-3-hexyne at 180 °C for 4−8 min. In most cases, about 0.2 wt % of antioxide Irganox 1010 (Ciba-Geigy) was also blended with the polymer to reduce the contribution of oxygen to the degradation and thereby increase the vinylidene group concentration in the final product.

Hydroboration Reaction. In a typical example, the hydroboration reaction was carried out under heterogeneous conditions by suspending 20 g of u-PP fine powder (u-PP-3) in 100 mL of THF. Slightly excess (0.5 g) 9-borabicyclononane (9-BBN) was added to the suspended solution to ensure the complete hydroboration reaction. The reaction mixture was stirred at 55 °C for 5 h before removing the polymer powder from solution by filtration.

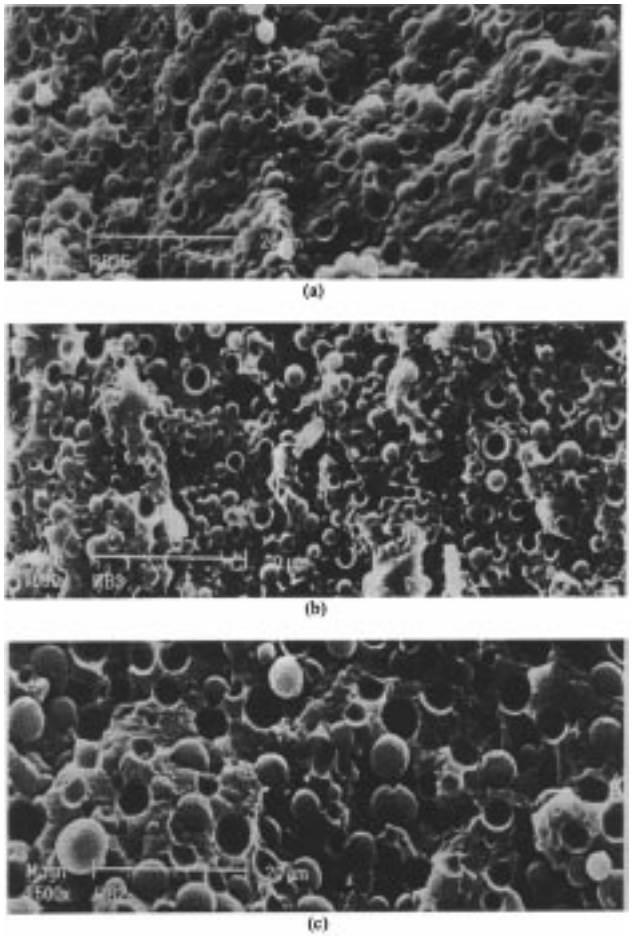

Figure 10. Comparison of three ternary PP/PP-*b*-SMA/Nylon 11 = 20/5/75 wt % blends, including (a) PP/PP-3-*b*-SMA-1/Nylon 11, (b) PP/PP-4-*b*-SMA-1/Nylon 11, and (c) PP/PP-9-*b*-SMA-1/Nylon 11. The magnification is 1500×.

Graft-from Reaction. The resulting 9-BBN terminated polypropylene (PP-9-BBN) was divided into several portions (1 g each); they were then subjected to the oxidation reaction by oxygen in the presence of MA or the mixture of MA and styrene, with various quantities shown in Table 2. The reaction was usually performed at ambient temperature by slowly adding a stoichiometric quantity of oxygen (vs borane) to the suspending polymer solution. After a certain reaction time (shown in Table 2), the radical reactions were terminated by precipitating the polymer mixture in 2-propanol. The product, isolated by filtration, was purified by Soxhlet extraction with acetone for 24 h. For a PP-*b*-SMA samples containing >3 wt % MA, such as PP-4-*b*-SMA-3, the reaction mixture was subjected to Soxhlet extraction with both refluxing xylene and acetone for 24 h to remove unreacted PP (0.12 g) and ungrafted SMA polymer (0.51 g). The xylene and acetone insoluble portion (2.014 g) is PP-4-*b*-SMA-3 diblock copolymer. In general, the graft efficiency was very high, and the major portion (>80%) of PP was converted to PP-*b*-SMA diblock copolymer.

Polymer Blending. All blending samples were prepared in a Brabender mixer PL2000 Plastic-Corder by mixing various polymers at 220 °C for 20 min. The mixture was then melt pressed to a film which was cryofractured in liquid N_2 to obtain an undistorted view representative of the bulk material. The surface of the cross section was sputtered with gold and then viewed with a Topcon International Scientific Intruments ISI-SX-40 using secondary electron imaging.

Conclusion

It has been both scientifically and industrially desired to develop maleic anhydride modified PP (PP-MA) with

a well-defined molecular structure for studying and improving the compatibility of PP in polymer blends. In this paper, we show a promising route to prepare PP-MA block copolymers with a controllable structure, i.e., PP molecular weight and MA units at the polymer chain end. The new PP-MA block copolymers provide detailed information about the effects of PP-MA structure to the compatibility of the reactive PP/Nylon blends. Specifically, the PP-*b*-SMA copolymer, with its high molecular weight PP segment and multiple MA units, offers excellent compatibility in PP-rich blends and almost no detectable benefit to Nylon-rich blends.

Acknowledgment. The authors thank the Petroleum Research Foundation for its financial support.

References and Notes

(1) Chung, T. C. *Macromolecules* **1988**, *21*, 865.
(2) Chung, T. C. *CHEMTECH* **1991**, *27*, 496.
(3) Kesti, M. R.; Coates, G. W.; Waymouth, R. M. *J. Am. Chem. Soc.* **1992**, *114*, 9679.
(4) Chung, T. C.; Jiang, G. J.; Rhubright, D. U.S. Pat. 5,401,805, 1995.
(5) Trivedi, B. C.; Culbertson, B. M. *Maleic Anhydride*; Plenum Press: New York, 1982.
(6) Garagnai, E.; Marzola, R.; Moro, A. *Mater. Plast. Elastomeri* **1982**, *5*, 298.
(7) Johnson, A. F.; Simms, G. D. *Composites* **1986**, *17*, 321.
(8) Fukushima, N.; Kitagawa, Y.; Sonobe, T.; Toya, H.; Nagai, H. Eur. Patent 78174.
(9) Ashley, R. J. *Adhesion* **1988**, *12*, 239.
(10) Felix, J. M.; Gatenholm, P. *J. Appl. Polym. Sci.* **1991**, *42*, 609.
(11) Myers, G. E. *J. Polym. Mater.* **1991**, *15*, 21.
(12) Majumdar, B.; Keskkula, H.; Paul, D. R. *Polymer* **1994**, *35*, 1386.
(13) Lambla, M. In *Comprehensive Polymer Science, First Supplement*; Allen, G., Ed.; Pergamon Press: New York, 1982.
(14) Priola, A.; Bongiovanni, R.; Gozzelino, G. *Eur. Polym. J.* **1994**, *30*, 1047.
(15) Ruggeri, G.; Aglietto, M.; Petragnani, A.; Ciardelli, F. *Eur. Polym. J.* **1983**, *19*, 863.
(16) Gaylord, N. G.; Mishra, M. K. *J. Polym. Sci., Polym. Lett. Ed.* **1983**, *21*, 23.
(17) Heinen, W.; Rosenmoller, C. H.; Wenzel, C. B.; de Groot, H. J. M.; Lugtenburg, J.; van Duin, M. *Macromolecules* **1996**, *29*, 1151.
(18) Lu, B.; Chung, T. C. *Macromolecles* **1998**, *31*, 5943.
(19) Chung, T. C.; Janvikul, W.; Bernard, R.; Jiang, G. J. *Macromolecules* **1993**, *27*, 26.
(20) Chung, T. C.; Janvikul, W.; Bernard, R.; Hu, R.; Li, C. L.; Liu, S. L.; Jiang, G. J. *Polymer* **1995**, *36*, 3565.
(21) Chung, T. C.; Lu, H. L.; Janvikul, W. *J. Am. Chem. Soc.* **1996**, *118*, 705.
(22) Chung, T. C.; Jiang, G. J. *Macromolecules* **1992**, *25*, 4816.
(23) Chung, T. C.; Jiang, G. J.; Rhubright, D. U.S. Patent 5,401,805, 1995.
(24) Bruah, S. D.; Laskar, N. C. *J. Appl. Polym. Sci.* **1996**, *60*, 649.
(25) Tsutsui, T.; Mizuno, A.; Kashiwa, N. *Polymer* **1989**, *30*, 428.
(26) Suwanda, D.; Lew, R.; Balke, S. T. *J. Appl. Polym. Sci.* **1988**, *35*, 1019.
(27) Coutinho, F. M. B.; Rocha, M. C. G.; Balke, S. T. In *Polymeric Materials Encyclopedia*; Salamone, J. C., Ed.; CRC Press: New York, 1996.
(28) Chung, T. C.; Lu, H. L.; Janvikul, W. *Polymer* **1997**, *38*, 1495.
(29) Russell, K. E.; Kelusky, E. C. *J. Polym. Sci., Part A: Polym. Chem.* **1988**, *26*, 2273.
(30) Sclavons, M.; Carlier, V.; DeRoover, B.; Franquinet, P.; Devaux, J.; Legras, R. J. *Appl. Polym. Sci.* **1996**, *62*, 1205.
(31) Brandrup, J.; Immergut, E. H. *Polymer Handbook*, 3rd ed.; Wiley-Interscience: New York, 1989.

MA990019Q